Temporal evolution of the pressure profile and mode behavior during internal reconnection events in the MAST spherical tokamak

H. Tojo[1)], M. Gryaznevich[2)], A. Ejiri[1)], A. Sykes[2)], Y. Takase[1)]

[1)]*Graduate School of Frontier Sciences, The University of Tokyo Kashiwa 277-8561, Japan*

[2)]*EURATOM/UKAEA Fusion Association, Culham Science Centre, OX14 3DB, UK*

(Received 15 October 2007 / Accepted)

Mode behaviors including non-linear development and pressure profiles during internal reconnection events are clarified in the MAST spherical tokamak. In a $q_0 > 1$ discharge, tearing mode is a trigger but non-linearity of modes is not confirmed. On the other hand, in a $q_0 < 1$ discharge, harmonics of a $m/n = 4/1$ mode of ∼22kHz are confirmed. Method for identification of poloidal mode in ST configuration is also given.

Keywords: IRE, spherical tokamak, bicoherence, poloidal mode, reconnection

DOI: 10.1585/pfr.1.001

1 Introduction

Internal Reconnection Events (IREs) have often been observed in spherical tokamaks (STs), limiting performance. IREs are MHD instabilities, which show mode growth of precursor and flatten pressure profile. They result in disruption in the worst case. Three-dimensional MHD simulations have shown that linear growth rate and mode number of pressure-driven modes depend on q_0 (safety factor at the magnetic axis) and β_t (toroidal beta), and that the non-linear coupling of linear modes leads to a large plasma deformation [1]. In this situation, magnetic reconnection occurs and core plasma energy is lost along the reconnected magnetic line. The relationship between the mode number (and its growth rate) and q_0 and β_t have not been clarified experimentally. Moreover non-linear coupling of modes just before IRE haven't been investigated in detail. In MAST [2], IREs appear in both $q_0 > 1$ and $q_0 < 1$ discharges and they often limit the achievable plasma beta in high-β regimes. Objectives of this study are to clarify mode number and its dependence on such parameters, and to confirm the existence of non-linear coupling.

2 Experimental setup

2.1 Mirnov coil array and identification of poloidal mode number

Mirnov coils (magnetic probes) are sensitive to external mode behavior and are employed to identify mode numbers. In MAST, magnetic coils are located along the toroidal direction (12ch at the most), and along the center column (40ch) and along the outboard (18ch at the most). In STs, the determination of poloidal mode numbers (m) is not easy because of the effects of non-circular magnetic flux surfaces and asymmetric magnetic field pitch angle. To overcome these problems we developed a method to evaluate the poloidal mode number and its intensity. Firstly, we assume helical filamentary currents, which generate magnetic fluctuations, on their resonant surface calculated from EFIT [3]. The poloidal positions of these filaments are decided by tracing a magnetic field line. The number of alternating positive and negative filament pairs coincides with the mode number. Figure 1 shows trajectories of magnetic lines at the surfaces $q = 1$, 1.5, 2, and 3. In this case, the initial poloidal angle ($\theta = 0$) is located at the outboard midplane. The poloidal location of each filament (i.e., marker filament) can be obtained from the intersection of the curve and an integer or a half integer toroidal turns (Fig. 1). The tangents of the lines become steep at $\theta \sim \pi$ because of the strong toroidal field at the inboard side. Therefore, poloidal distribution of the filaments is asymmetric, and most of them tend to locate at the high field side. Number of filaments (and their rational surface), current amplitude and the poloidal location of the initial filament were obtained from the best fit to the measured Mirnov coil signals. Performing fittings at each timing, we can derive poloidal rotation and amplitude growth of the mode. However in this report we used band-passed signals and assume single mode distortion located at a rational surface to study the role of the dominant mode. Note that this model is appropriate for localized rational modes, such as tearing modes.

2.2 Measurements of soft X-ray profile

Soft X-ray radiation (SXR) is useful to study MHD phenomena and it includes information on internal mode struc-

author's e-mail: tojo@fusion.k.u-tokyo.ac.jp

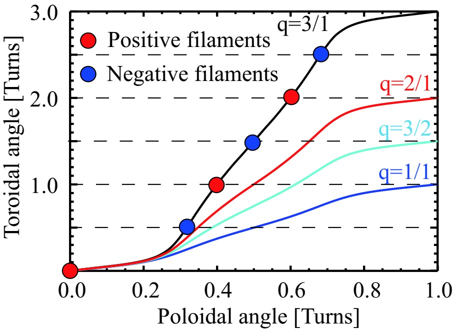

Fig. 1 Trajectory of the magnetic field lines at the rational surfaces q =1, 1.5, 2, 3. Poloidal angles of filaments are obtained from the intersections between the traces and horizontal lines with intervals of half integer turns.

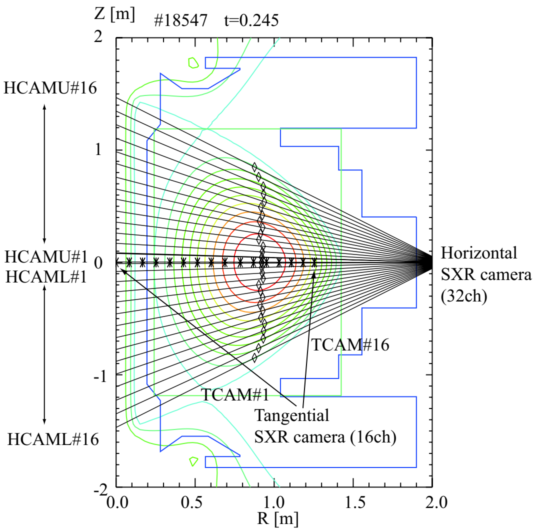

Fig. 2 Configuration of horizontal (sight lines) and tangential (asterisk) SXR cameras.

ture. Horizontal (32ch) and tangential (16ch) SXR cameras are employed and their sight lines are shown in Fig. 2. To compare behavior of SXR, q (calculated from EFIT) and (electron) pressure profile (measured by Thomson scattering), sight lines of each SXR channel are labeled by the minimum poloidal flux (ψ) obtained by the EFIT. In other words, along each sight line we determine the minimum of the ψ (symbols in Fig. 2) and corresponding radial position R.

2.3 Analysis using bispectrum to show non-linear coupling

To clarify non-linear development of the IRE precursors we performed bispectrum analysis which is a Fourier analysis for three wave interaction and used frequently in turbulence analysis [4] [5]. Generally, auto bispectrum is defined as

$$B(f_1, f_2) = \langle X(f_1)X(f_2)X^*(f_3)\rangle \tag{1}$$

where $f_3 = f_1 + f_2$ and $X(f)$ is a Fourier components of signal $x(t)$. To evaluate the degree of nonlinear coupling for each frequency component, following normalized auto bispectrum is commonly used as

$$b^2(f_1, f_2) = \frac{|B^2(f_1, f_2)|^2}{\langle|X(f_1)X(f_2)|^2\rangle\langle|X^*(f_3)|\rangle} \tag{2}$$

If there is a strong non-linear relation among f_1 and f_2, b^2 becomes large (nearly 1). We analyzed Mirnov coils data for understanding non-linear development in IRE precursor. To obtain accurate bicoherence, many ensembles should be averaged. In MAST, there are twelve (at the most) toroidal Mirnov coils around the center column at same poloidal position. We employed these coil data to perform the ensemble averaging. Total bicoherence is defined as

$$B^2_{tot} = \sum_{f_1, f_2} B^2(f_1, f_2) \tag{3}$$

which represents quantitative measure of the non-linear coupling.

3 IRE discharges

3.1 IRE with $q_0 > 1$

A typical discharge with $q_0 > 1$ and $\beta_t \sim 9\%$ is shown in Fig. 3. Increase of the plasma current (I_p) and drop of the electron density from interferometer were observed. The increase on the emission of D_α indicates interaction between the plasma and the vacuum vessel due to the loss of the plasma. One of unique characteristics of the events is that SXR radiation profile shows propagation of the drop starting from the area of fluctuations (precursor). This IRE has precursor not only in SXR radiation, but also in the Mirnov coil signals. The position of reconnection is close to HCAMU♯12 (R ~1.25) because HCAMU♯13-15 increase, while HCAMU♯3-11 decrease after $t \sim 0.2545$ (see arrows in Fig. 3). We executed the fitting code to determine the mode number. Here we applied band-pass (1-5kHz) filtering to the time integrated Mirnov signals. An example of the fitting is shown in Fig. 4. The squares represent the Mirnov coil data at $t = 0.24720$ and the line shows a fitted curve assuming only 2/1 mode (filaments) at the rational surface $q = 2$. They show good agreement. Figure 4 indicates time evolution of the calculated helical filament current (a), poloidal angle of a filament (b) and, fitting error (c). As described in 2.1, filament current reflects mode intensity and it can be used to derive the growth time. From $t \sim 0.241$ the filament current increases exponentially, indicating a linear growth. Time constant (τ_{fil}) of this growth is about 6 ms. The phase of the filament decreases continuously, showing a poloidal rotation of the filaments. The error of the fitting is represented by the normalized residual error χ^2. When χ^2 is less than 10, the quality of the fitting is acceptable in the present analysis. We preformed

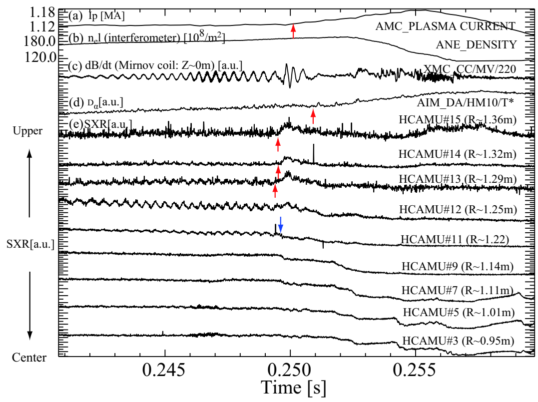

Fig. 3 IRE in discharge with $q_0 > 1$. (a): Plasma current [kA] (b): Line integrated electron density [$/m^2$] (c): dB/dt from Mirnov coil [a.u.] (d) Emission of D_α [a.u.] (e): SXR radiation [a.u.] on horizontal SXR camera from upper to center side of the plasma.

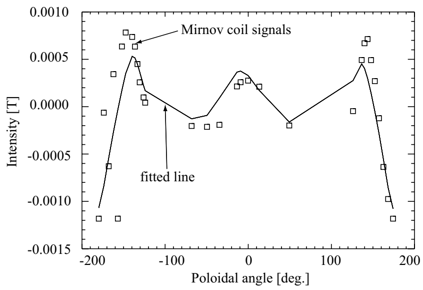

Fig. 4 Integrated Mirov coils signal (1-5kHz) and fitted curve of the model assuming only m/n =2/1 mode for ♯18547 at t = 0.24720s. The origin of poloidal angle is the magnetic axis determined by the EFIT.

the bispectrum calculation on the toroidal Mirnov signals ($\phi = 10°, 50°, 70°, 110°, 130°, 170°, 230°, 290°$) with 250kHz sampling rate in order to check non-linearity. The number of ensemble is 8 and data points per one ensemble is 750. There is strong bicoherence around (f_1, f_2) ~ (40kHz, 40kHz) indicating harmonic coupling with itself but these modes are localized near the centre of the plasma. Therefore the 2/1 mode was localized near the reconnection position and can be a candidate for the trigger of this IRE.

3.2 IRE with $q_0 < 1$

In the case of $q_0 < 1$, IRE should be distinguished from sawtooth oscillation, which is instability at $q = 1$ rational surface. In this study, IRE is defined as the instability with mode couplings and/or often accompanied by a collapse at a rational surface except for $q = 1$ surface. Figure 6 shows an IRE discharge with $q_0 < 1$. This IRE doesn 't terminate the plasma but reduces β_t significantly. The position of the reconnection is around HCAMU♯14 (R ~1.45m). However, the area with strong oscillation is closed to HCAMU♯12(R ~1.2-1.3m) and the phase differ-

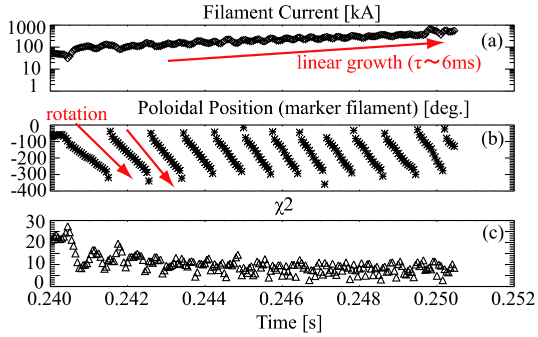

Fig. 5 Time evolution of the fitting parameters for ♯18547. (a): Filament current [kA] (b): Poloidal angle of the one chosen marker filament to understand poloidal rotation. (c): χ^2 (error of the fittings)

ence between HCAMU♯9 and 11 is significant. Therefore, this is tearing mode and the resonant surface is at R ~ 1.24 – 1.28m. The fitting code doesn't work well on this shot because the calculated position of the resonant surface (from EFIT) is presumably not good. However, as is indicated in section 2.1, the number of filaments (model of the mode) on outboard side is very few because of low aspect ratio configuration. Therefore the poloidal mode number can be estimated roughly by counting peaks along the centre stack and adding one for outboard filament. In this way m/n =2/1 is confirmed for this q_0 <1 discharge. Note that it is difficult to derive the growth time and rotation w/o the fitting. The width of 2/1 mode seems increasing, as shown by SXR radiation from outer side, for example, HCAMU♯14 from t ~ 0.392s. In addition, Mirnov coils show another high frequency mode (~22kHz). Unfortunately, there is no strong cross correlation between this high frequency mode and any of SXR channels, and the position of this mode is not clear from SXR signals. However, poloidal mode number (m) is presumably 4 and toroidal mode (n) is 1. These mode numbers are determined by the Mirnov coil arrays. Therefore, this mode is localizes at the edge. To clarify the relationship between these modes (i.e., 3kHz, and 22kHz), bicoherence spectrum is calculated. For t = 0.389 – 0.392 there is no significant coupling between the two modes. Instead of that, 4/1 mode (~22kHz) shows second and third harmonic mode (~45kHz, ~68kHz). Figure 7 shows the result in later period t = 0.392 – 0.395s. These frequency are localized on the frequency space and sharp coherence disappears, but broad bicoherence in the region $f_1 + f_2$ <50kHz appears, suggesting non-linear coupling among a lot of modes. This is consistent with the non-linear phase of the MHD simulation in the reference [1]. The total squared bispectrum (duration of ensemble is~3ms) at these two periods show a siginificant increase of about 50 times. However, we cannot decide which mode is a trigger of this IRE because the position of the high frequency mode has not been identified.

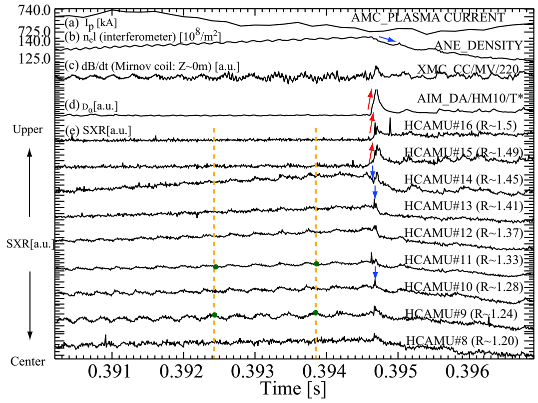

Fig. 6 IRE in a discharge with q_0 <1. (a): Plasma current [kA] (b): Line integrated electron density [$/m^2$] (c): dB/dt from Mirnov coil [a.u.] (d): Emission of D_α[a.u.] (e): SXR radiation [a.u.] on horizontal SXR camera from upper to center （SXR signals for midplane to upper chords.） side of the plasma.

4 IRE drive

To understand the drive of IRE is important for the prevention. For a comparison with the reference [1], which suggested pressure-driven mode as the source of the instabilities, we evaluated pressure gradient for some IRE discharges. Figure 8 shows time evolutions of a correlation between magnetic shear (S) and pressure gradient (dP/dr) for thirteen shots, where magnetic shear defined as $S = (r/q) \cdot dq/dr$. These two parameters are calculated by kEFIT which takes into account pressure profile from the Thomson scattering profile. Red circles represent the values just before each IRE. IRE occurs when pressure gradient exceed critical value, which becomes high at high shear. Note that although there are many shots showing increase of the gradient by the time of IRE, some shots don't show such behavior under the result from the kEFIT.

5 Summary and conclusion

In this paper, IREs in the MAST plasma are studied using a filament model, in which low aspect ratio effects are taken into account. In the case of $q_0 > 1$ no mode coupling concerning to IRE are observed but the growth of the 2/1 tearing mode with $\tau \sim 6ms$ is confirmed. The mode triggers a collapse. In the IRE with $q_0 < 1$, slow growth of the 2/1 tearing mode is observed and 2nd and 3rd harmonic from a 4/1 mode, (f_1, f_2) ~(22kHz, 22kHz) and (f_1, f_2) ~(22kHz, 44kHz), are confirmed in Mirnov coil signals. After that, these bicoherence peaks disappear and broad bicoherence on a range of $f_1 + f_2$ <50kHz is observed. This is consistent with the time evolution of each mode in [1]. Although we haven't found a clear evidence of non-linear development causing an IRE followed by collapse, the 2/1 mode may trigger the collapse. To find out the source of IRE traces

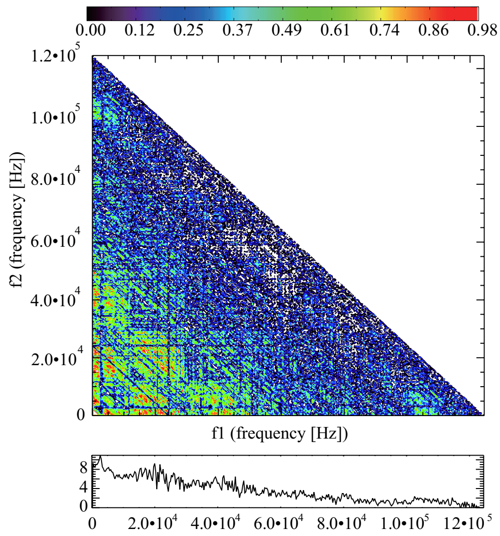

Fig. 7 ♯18501 Bicoherence spectrum (t = 0.392 – 0.395) of the toroidal Mirnov coils (top Fig.) and power spectrum on logarithmic scale (bottom Fig.).

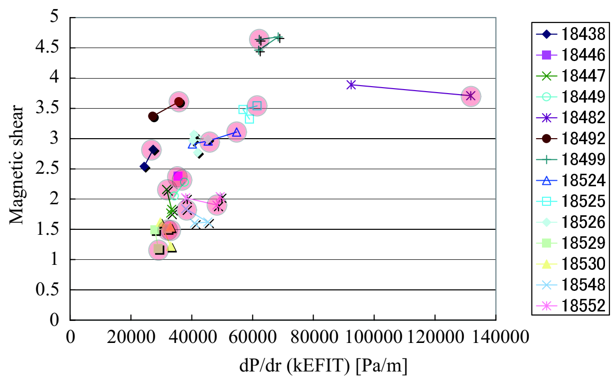

Fig. 8 Trace of magnetic shear (S) and pressure gradient from the kEFIT ressult at q = 2 rational surface before (0 ~ 21ms) IRE. Same symbol shows same shot. The red shaded circles indicate just before the IRE.

of pressure gradient and magnetic shear. Critical pressure gradient at q = 2 increases with magnetic shear suggesting pressure-driven nature of IREs.

6 Acknowledgment

This work was supported by JSPF Grant-in-Aid for Scientific Research 16106013.

[1] N. Mizuguchi et al., Phys. Plasmas **7** (2000) 940.
[2] B. Lloyd et al., Nucl. Fusion **43** (2003) 1665.
[3] L. Lao et al., Nucl. Fusion **25** (1985) 1611.
[4] Y.C. Kim and E.J. Powers, Phys. Fluids **21** (1978) 1452.
[5] Y. Nagashima et al., Plasma Phys. Control. Fusion **49** (2007) 1611.